Measurement of the 20 and 90 keV Resonances in the $^{18}O(p, \alpha)^{15}N$ Reaction via the Trojan Horse Method

M. La Cognata,[1] C. Spitaleri,[1,*] A. M. Mukhamedzhanov,[2] B. Irgaziev,[3] R. E. Tribble,[2] A. Banu,[2] S. Cherubini,[1] A. Coc,[4] V. Crucillà,[1] V. Z. Goldberg,[2] M. Gulino,[1] G. G. Kiss,[5] L. Lamia,[1] J. Mrazek,[6] R. G. Pizzone,[1] S. M. R. Puglia,[1] G. G. Rapisarda,[1] S. Romano,[1] M. L. Sergi,[1] G. Tabacaru,[2] L. Trache,[2] W. Trzaska,[7] and A. Tumino[1]

[1]*INFN Laboratori Nazionali del Sud & DMFCI Università di Catania, 95123 Catania, Italy*
[2]*Cyclotron Institute, Texas A&M University, College Station, 77843 Texas, USA*
[3]*GIK Institute of Engineering Sciences and Technology, Topi (23640), NWFP Pakistan*
[4]*CSNSM, CNRS/IN2P3 Universitè Paris Sud, F-91405 Orsay, France*
[5]*ATOMKI, H-4001 Debrecen, Hungary*
[6]*Nuclear Physics Institute of ASCR, 25068 Rez near Prague, Czech Republic*
[7]*Physics Department, University of Jyväskylä, FIN-40014 Jyväskylä, Finland*

(Received 13 June 2008; published 7 October 2008)

The $^{18}O(p, \alpha)^{15}N$ reaction is of primary importance in several astrophysical scenarios, including fluorine nucleosynthesis inside asymptotic giant branch stars as well as oxygen and nitrogen isotopic ratios in meteorite grains. Thus the indirect measurement of the low energy region of the $^{18}O(p, \alpha)^{15}N$ reaction has been performed to reduce the nuclear uncertainty on theoretical predictions. In particular the strength of the 20 and 90 keV resonances has been deduced and the change in the reaction rate evaluated.

DOI: 10.1103/PhysRevLett.101.152501 PACS numbers: 24.10.−i, 25.40.Hs, 26.20.−f, 27.20.+n

Understanding fluorine production would make predictions on asymptotic giant branch (AGB) star nucleosynthesis more accurate. The AGB stage represents the final nuclosynthetic phase in low and intermediate mass stars. AGB stars play an extremely important role in astrophysics because heavy elements along the stability valley are produced in their interiors through slow neutron captures (*s* process). ^{19}F can be produced during the thermal pulse that is ignited in the ^{4}He-rich intershell region, following the ingestion of the ^{13}C pocket. The subsequent third dredge-up (TDU) episode mixes the products of shell flash He-burning, including fluorine, and *s* process nuclei to the outer layers. Therefore ^{19}F abundance constitutes a key parameter to constrain AGB star models [1]. Anyway, if the theoretical abundances are compared to the observed ones, a remarkable discrepancy shows up because the largest ^{19}F abundances cannot be matched for the typical $^{12}C/^{16}O$ ratios [1]. A possible way to explain ^{19}F abundance and several related observables (such as isotopic ratios in meteorite grains [2]) can be linked to ^{18}O as the $^{18}O(p, \alpha)^{15}N$ reaction represents the main ^{15}N production channel, both in the intershell region and at the bottom of the convective envelope [1,2]. During the thermal pulse ^{15}N is burnt to ^{19}F via the $^{15}N(\alpha, \gamma)^{19}F$ reaction. Thus a larger $^{18}O(p, \alpha)^{15}N$ reaction rate would lead to an increase of the ^{19}F supply as well as to an enrichement of ^{15}N in the stellar surface, which would play a key role to explain the long-standing problem of the $^{14}N/^{15}N$ ratio in meteorite grains ([2] and references therein).

The $^{18}O(p, \alpha)^{15}N$ reaction has been the subject of several experimental investigations [3,4] and many features are known from spectroscopic studies [5–8]. Nevertheless the reaction rate for the process has a considerable uncertainty [9]. In the 0–1000 keV energy range, where 9 resonances occur, the reaction rate is essentially determined by the 20, 144, and the 656 keV resonances [9]. With regard to the 20 keV resonance, its strength is known only from spectroscopic measurements performed through the transfer reaction $^{18}O(^{3}He, d)^{19}F$ [6] and the direct capture reaction $^{18}O(p, \gamma)^{19}F$ [7]. Such estimates, which are based on the deduced spectroscopic factors, are strongly model dependent (being connected to the adopted optical model potentials) and affected by large and not-well-defined uncertainties. An additional important source of uncertainty on the reaction rate is connected with the determination of the resonance energy [6]. Furthermore the spin and parity of the 8.084 MeV level in ^{19}F (corresponding to a 90 keV resonance in the $^{18}O(p, \alpha)^{15}N$ cross section) has not been established. The uncertainties on nuclear physics inputs have made astrophysical predictions far from conclusive [2].

In order to reduce the nuclear uncertainties affecting the reaction rate estimate we have performed an experimental study of the $^{18}O(p, \alpha)^{15}N$ reaction by means of the Trojan horse method (THM), which is an indirect technique to measure the relative energy-dependence of a charged-particle reaction cross section at energies well below the Coulomb barrier ([10,11] and references therein). The cross section of the relevant $A + x \rightarrow c + C$ reaction is deduced from a suitable $A + a(x \oplus s) \rightarrow c + C + s$ process, performed in quasifree (QF) kinematics. The beam energy is chosen larger than the Coulomb barrier for the interacting nuclei, so the breakup of nucleus *a* (the so-called *Trojan-horse*) takes place inside the *A* nuclear field.

Therefore, the cross section of the $A + x \rightarrow c + C$ reaction is not suppressed by the Coulomb interaction of the target-projectile system.

In a previous investigation, carried out at the Cyclotron Institute, Texas A&M University, Texas (USA) [12], the $^{18}O(p, \alpha)^{15}N$ reaction has been measured via the THM through the $^{2}H(^{18}O, \alpha^{15}N)n$ process in the 0–1000 keV $^{18}O - p$ relative energy range. For the first time the energy region below 70 keV had been investigated. In the present work we focus on a new study of the $^{18}O(p, \alpha)^{15}N$ reaction by means of the same THM process. The aim is to span the $^{18}O - p$ relative energy region below 250 keV with an improved energy resolution, in order to deduce resonance parameters and J^{π} values of the 8.014 and 8.084 MeV ^{19}F levels. The experiment was performed at Laboratori Nazionali del Sud, Catania (Italy). The SMP Tandem Van de Graaff accelerator provided the 54 MeV ^{18}O beam impinging onto thin self-supported deuterated polyethylene (CD_2) targets. The detection setup consisted of a telescope (A), devoted to ^{15}N detection, made up of an ionization chamber and a silicon position sensitive detector (PSD A) on one side with respect to the beam direction, and three additional silicon PSD's (B, C and D) on the opposite side. Angular conditions were selected in order to maximize the expected QF contribution. Channel selection has been accomplished by gating on the $\Delta E - E$ 2D spectra to select the nitrogen locus.

Compelling evidence for the occurrence of the QF mechanism is given by the shape of measured momentum-distribution, if it follows the shape of the deuteron wave function. In the analysis, the theoretical distribution, given by the square of the Hulthén wave function in momentum space in the plane wave approximation [11], is superimposed onto the experimental one. The good agreement demonstrates that the QF mechanism is present and dominant in the $|p_3| < 50$ MeV/c neutron momentum range. Thus, in the following analysis only the phase space region for which the $|p_3| < 50$ MeV/c condition is satisfied is taken into account.

Angular distributions for the $^{18}O(p, \alpha)^{15}N$ reaction were extracted as discussed in [11]. They were used to perform the necessary validity test on the deduced cross section and to infer the spin-parity for the states. The α emission angles in the c.m. system ($\theta_{\text{c.m.}}$), covered in the present experiment, were about $\theta_{\text{c.m.}} = 0°$–$60°$, $\theta_{\text{c.m.}} = 40°$–$110°$ and $\theta_{\text{c.m.}} = 90°$–$150°$ for the A-B, A-C, and the A-D detector coincidences, respectively. The presence of an overlap region allowed for relative normalization between the cross sections deduced from each couple. Angular distributions were extracted for several energies, focusing, in particular, on the 20, 90, and 143.5 keV resonances. The results are displayed in Fig. 1 where the experimental data are given as filled circles (20), squares (90), and triangles (143.5 keV). Errors on the half-off-energy-shell (HOES) [11] cross section $\frac{d\sigma}{d\Omega}$ account for statistics and for the deconvolution of the single resonance contributions. The

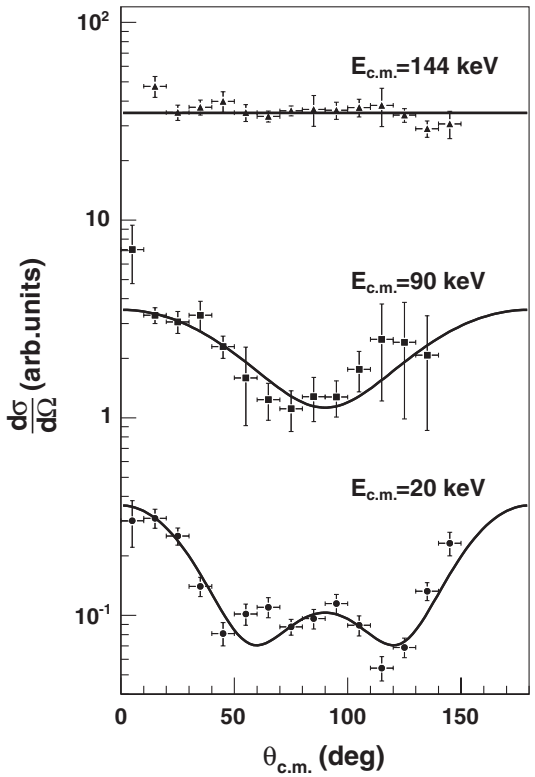

FIG. 1. Experimental angular distributions for the $^{18}O(p, \alpha)^{15}N$ reaction for the three resonances in the 0–250 keV energy range. The full lines come from the fitting with the curve of Eq. (1).

error on $\theta_{\text{c.m.}}$ represents the width of each bin (chosen in order to have reasonable statistical precision).

From Fig. 1 it turns out that the $J^{\pi} = \frac{1}{2}^{+}$ assignment for the 143.5 keV resonance is confirmed, the angular distribution for that level being isotropic (see Fig. 1). This result represents a cross check of the method, since we are able to reproduce the angular distribution for a well-known resonance. Therefore we extracted the angular distribution for both the 90 and 20 keV resonances. A fit of the experimental data was performed by

$$\frac{d\sigma}{d\Omega_{\text{c.m.}}} = \frac{d\sigma}{d\Omega_{\text{c.m.}}}(90°)(1 + A_2(E)\cos^2\theta + A_4(E)\cos^4\theta + \ldots + A_{2L}(E)\cos^{2L}\theta), \quad (1)$$

where L is the smallest among the spin J of the formed compound nucleus and the angular momentum l quantum numbers in the entrance and the exit channels [13]. The best fit for the 90 keV resonance is achieved for $L = 1$ ($\tilde{\chi}^2 = 0.67$); thus, we infer a spin for the 8.084 MeV excited state of ^{19}F of $\frac{3}{2}$. We consider that this L value corresponds to the angular momentum in the exit channel, because of considerations on the proton width of this level, and the parity to be positive (the ^{15}N ground state being $\frac{1}{2}^{-}$). For the 20 keV resonance, the best fit is obtained for $L = 2$ ($\tilde{\chi}^2 = 3.11$), supporting the $J^{\pi} = \frac{5}{2}^{+}$ spin-parity

assignment for the ^{19}F excited state at 8.014 MeV (see [6,8]). In the extraction of the angular distributions the $^{18}O - p$ relative energy is kept fixed thus preventing possible bias caused by the HOES nature of the deduced cross section. The HOES effect might be expressed by a constant renormalization factor, and therefore the angular distributions are given in arbitrary units in Fig. 1.

The extracted HOES differential cross section has been integrated in the whole angular range. It was assumed that in the region where no experimental angular distributions are available, their trend is given by the fit of Eq. (1). The resulting ^{2}H(^{18}O, α^{15}N)n reaction cross section is shown in Fig. 2 (full circles). The experimental energy resolution turned out to be about 40 keV (FWHM), in agreement with the value predicted by Monte Carlo simulations. Horizontal error bars represent the integration bin while the vertical ones arise from statistical uncertainty and angular distribution integration. Indeed, because of the limited energy resolution, resonances were not well resolved; thus, each contribution to the reaction yield had to be disentangled when extracting angular distributions. The solid line in the figure is the sum of three Gaussian functions to fit the resonant behavior and a straight line to account for the nonresonant contribution to the cross section. This fit was performed with the sole aim of extracting the resonance energies: $E_{R_1} = 19.5 \pm 1.1$ keV, $E_{R_2} = 96.6 \pm 2.2$ keV, and $E_{R_3} = 145.5 \pm 0.6$ keV (in fair agreement with the ones reported in the literature [9]) and to deduce the peak values of each resonance: $N_1 = 138 \pm 8$, $N_2 = 82 \pm 9$, and $N_3 = 347 \pm 8$ (arbitrary units). The peak values were used to derive the resonance strengths $\omega\gamma$ that are the relevant parameters for astrophysical application in the case of narrow resonances [9]. The THM cross section for the $A + a(x \oplus s) \rightarrow c + C + s$ reaction proceeding through a resonance F_i in the subsystem $F = A + x = C + c$ is [11,14]

$$\frac{d^2\sigma}{dE_{Cc}d\Omega_s} \propto \frac{\Gamma_{(Cc)_i}(E)|M_i(E)|^2}{(E - E_{R_i})^2 + \Gamma_i^2(E)/4}. \quad (2)$$

Here, $M_i(E)$ is the direct transfer reaction amplitude for the binary reaction $A + a \rightarrow F_i + s$ populating the resonant state F_i with the resonance energy E_{R_i}, E is the $A - x$ relative kinetic energy related to E_{Cc} by the energy conservation law, $\Gamma_{(Cc)_i}(E)$ is the partial resonance width for the decay $F_i \rightarrow C + c$ and Γ_i is the total resonance width of F_i. The appearance of the transfer reaction amplitude $M_i(E)$ instead of the entry channel partial resonance width $\Gamma_{(Ax)_i}(E)$ is the main difference between the THM cross section and the cross section for the resonant binary subreaction $A + x \rightarrow C + c$ [11,14]. On the other hand, the resonance parameters deduced by means of the THM are not affected by the electron screening, distorting the direct S factor at the astrophysically relevant energies [15].

The peak THM cross section taken at the E_{R_i} resonance energy for the (p, α) reaction $A + x \rightarrow C + c$ is given by

$$N_i = 4\frac{\Gamma_{\alpha_i}(E_{R_i})M_i^2(E_{R_i})}{\Gamma_i^2(E_{R_i})}, \quad (3)$$

where $\Gamma_{Cc_i}(E) \equiv \Gamma_{\alpha_i}(E)$. In this work we did not extract the absolute value of the cross section. The proton and alpha partial widths for the third resonance at 143.5 keV are well known [9]; thus, we can determine the alpha partial width and the strength for the first and second resonances from the ratio of the peak values of the THM cross sections

$$(\omega\gamma)_i = \frac{\omega_i}{\omega_3}\frac{\Gamma_{p_i}(E_{R_i})}{|M_i(E_{R_i})|^2}\frac{|M_3(E_{R_3})|^2}{\Gamma_{p_3}(E_{R_3})}\frac{N_i}{N_3}(\omega\gamma)_3, \qquad i = 1, 2. \quad (4)$$

Here, $(\omega\gamma)_i = \omega_i\Gamma_{\alpha_i}(E_{R_i})\Gamma_{p_i}(E_{R_i})/\Gamma_i(E_{R_i})$ is the ith resonance strength, $\omega_i = \hat{J}_i/(\hat{J}_A\hat{J}_x)$ is the statistical factor, $\hat{J} = 2J + 1$, J_i is the spin of the ith resonance and J_A, J_x are the spins of A and x, respectively. When determining $(\omega\gamma)_i$ the effect of energy resolution in our experiment has been taken into account. The electron screening gives a negligible contribution around 144 keV (4% maximum [15]); thus, no systematic uncertainty is introduced by normalizing to the third resonance. In the plane wave approximation $M_i \approx \varphi_a(p_{sx})W_{Ax}(\mathbf{p}_{Ax})$, where $\varphi_a(p_{sx})$ is the Fourier transform of the s-wave radial $s - x$ bound wave function, p_{sx} is the $s - x$ relative momentum, and $W_{Ax} = \langle I_{Ax}^{F^*}|V_{Ax}|\mathbf{p}_{Ax}\rangle$ is the form factor for the synthesis $A + x \rightarrow F_i$, $I_{Ax}^{F^*}$ is the overlap function of the bound state wave functions of A, x and the resonant wave function of F^*, $\mathbf{p}_{Ax}$ is the $A - x$ relative momentum. In practical calculation we approximated $I_{Ax}^{F_i}$ by $S_i^{1/2}\varphi_{(Ax)_i}$, where S_i is the spectroscopic factor for configuration $F_i = A + x$ and $\varphi_{(Ax)_i}$ is the

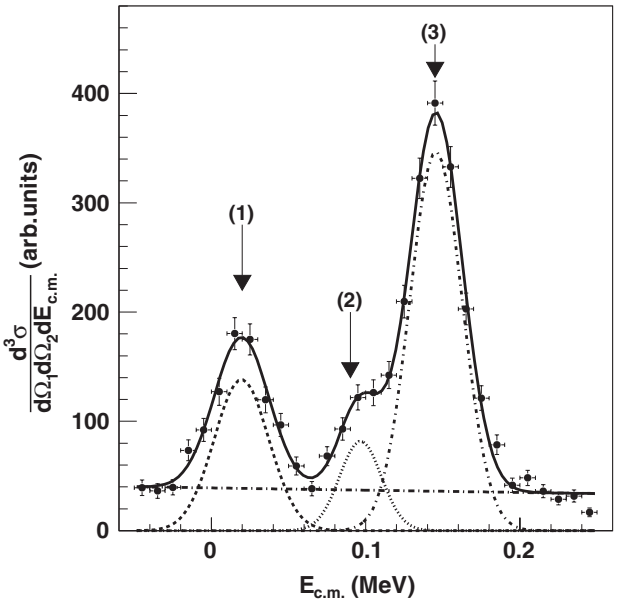

FIG. 2. Cross section of the TH reaction (full circles). (1), (2), and (3) refer to the 8.014, 8.084, and 8.138 MeV ^{19}F levels. The full line represent the result of a fit including three Gaussian curves and a 1st order polynomial.

single-particle bound-state type wave function describing the resonance state F_i. Since in Eq. (4) only the $\frac{\Gamma_{p_i}(E_{R_i})}{|M_i(E_{R_i})|^2}$ ratios show up, the dependence on spectroscopic factors and proton widths is completely removed and, as a consequence, $(\omega\gamma)_i$ is connected to $(\omega\gamma)_3$ through the easily calculable ratios of the single-particle widths to the form factors W_{Ax}. If $(\omega\gamma)_3$ is taken from [16], by means of Eq. (4) one gets $(\omega\gamma)_1 = 8.3^{+3.8}_{-2.6} \times 10^{-19}$ eV, which is well within the upper and lower limits given by NACRE, $6^{+17}_{-5} \times 10^{-19}$ eV [9]. While NACRE recommended value is based on varius kinds of estimates, the present result is obtained from experimental data; thus, the accuracy of the deduced resonance strength has been greatly enhanced. The largest contribution to the error is due to the uncertainty on the resonance energy, while statistical and normalization errors sum up to about 9.5%. With a similar approach we have obtained $(\omega\gamma)_2 = (1.76 \pm 0.33) \times 10^{-7}$ eV (statistical and normalization errors $\sim$13%) for the 90 keV resonance, in good agreement with the strength given by NACRE, $(1.6 \pm 0.5) \times 10^{-7}$ eV [9]. This gives us confidence in the theory used in the THM allowing for a cross check of the method.

By using the narrow resonance approximation [9], which is fulfilled for the resonances under investigation, the reaction rate has been deduced and compared with the one reported in NACRE [9]. In Fig. 3 the ratio of the THM reaction rate to the NACRE one for the ^{18}O$(p, \alpha)^{15}$N is shown as a full black line. The dot-dashed and dotted black lines represent the upper and lower limits, respectively, allowed by the experimental uncertainties. In the low temperature region (below $T_9 = 0.03$, Fig. 3) the reaction rate can be about 35% larger than the one given by NACRE (full red line), while the indetermination is greatly reduced with respect to the NACRE one (dot-dashed and dotted red lines mark the upper and lower limits, Fig. 3). Those temperatures are typical of the bottom of the convective envelope; thus, an increase of this reaction rate might have important consequences on the cool bottom process [2] and, in turn, on the surface abundances and isotopic ratios in AGB stars. The 8.084 MeV excited state of ^{19}F (corresponding to the 90 keV resonance) provides a negligible contribution to the reaction rate in agreement with previous estimate [6].

In conclusion, in this Letter we demonstrated, for the first time, the power of indirect THM which allowed to determine the strength of the low-lying 20-keV resonance in ^{19}F, elusive for any direct technique. This resonance plays an important role in the determination of the reaction rates of the key astrophysical reaction ^{18}O$(p, \alpha)^{15}$N. We also presented a new way of determination of the resonance strength by measuring the relative strengths of the known and unknown resonances and using the half-off-shell R matrix to determine the strength of the unknown resonance avoiding information about the spectroscopic factors. The parameters of the 20 keV resonance in the

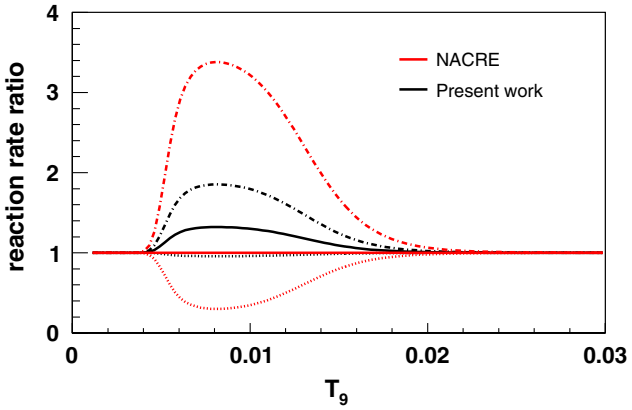

FIG. 3 (color online). Ratio of the THM reaction rate (full black line) to the NACRE one [9]. For comparison, the NACRE rate is shown as a red line. The dot-dashed and dotted lines show the upper and lower limits allowed by experimental uncertainties.

^{18}O$(p, \alpha)^{15}$N reaction relevant for astrophysics together with those for the nearby resonances could be extracted and importantly their uncertainty was strongly reduced (by a factor $\sim$8.5), thanks to the newly developed approach, which is based on experimental data in contrast to the NACRE one that relies on varius kinds of estimate. Indeed, in Eq. (4) only the ratio of the model dependent parameters in Eq. (3) shows up, thus systematic uncertainties cancel out. In addition, our results are not affected by the electron screening, which can enhance the cross section by a factor $\gtrsim 2.4$ at 20 keV [15], thus spoiling any direct measurement of this resonance. At higher temperatures, higher energy resonances in the ^{18}O$(p, \alpha)^{15}$N reaction can play a role. Their study will be the subject of forthcoming works.

*Spitaleri@lns.infn.it

[1] M. Lugaro *et al.*, Astrophys. J. **615**, 934 (2004).
[2] K. M. Nollett *et al.*, Astrophys. J. **582**, 1036 (2003).
[3] H. B. Mak *et al.*, Nucl. Phys. **A304**, 210 (1978).
[4] H. Lorentz-Wirzba *et al.*, Nucl. Phys. **A313**, 346 (1979).
[5] K. Yagi *et al.*, J. Phys. Soc. Jpn. **17**, 595 (1962).
[6] A. E. Champagne *et al.*, Nucl. Phys. **A457**, 367 (1986).
[7] M. Wiescher *et al.*, Nucl. Phys. **A349**, 165 (1980).
[8] C. Schmidt *et al.*, Nucl. Phys. **A155**, 644 (1970).
[9] C. Angulo *et al.*, Nucl. Phys. **A656**, 3 (1999).
[10] C. Spitaleri *et al.*, Phys. Rev. C **60**, 055802 (1999).
[11] M. La Cognata *et al.*, Phys. Rev. C **76**, 065804 (2007).
[12] M. La Cognata *et al.*, J. Phys. G **35**, 014014 (2008).
[13] R. D. Evans, *The Atomic Nucleus* (McGraw-Hill, New York, 1969).
[14] A. M. Mukhamedzhanov *et al.*, J. Phys. G **35**, 014016 (2008).
[15] H. J. Assenbaum *et al.*, Z. Phys. A **327**, 461 (1987).
[16] H. W. Becker *et al.*, Z. Phys. A **351**, 453 (1995).